Research Square

Preprints are preliminary reports that have not undergone peer review.
They should not be considered conclusive, used to inform clinical practice,
or referenced by the media as validated information.

Contrasting diel patterns of organic and inorganic carbon dynamics in coraliths, rhodoliths, and colonized artificial substrates in a tropical reef system

Dairo H. Marin-Casas1
Universidad de los Andes
Carlos E. Gómez
Universidad de los Andes
Guilherme H. Pereira-Filho
Universidade Federal de São Paulo
Juan Armando Sánchez
juansanc@uniandes.edu.co

Universidad de los Andes

Research Article

Keywords: Colombian Caribbean, calcification, metabolic coupling, photosynthesis, respiration, Siderastrea radians, rhodoliths, coraliths

Posted Date: June 9th, 2026

DOI: https://doi.org/10.21203/rs.3.rs-9867136/v1

License: This work is licensed under a Creative Commons Attribution 4.0 International License.
Read Full License

Additional Declarations: No competing interests reported.

Abstract

Understanding how calcifying benthic systems contribute to short-term carbon dynamics is essential for predicting their role in shallow tropical ecosystems under environmental change. We compared diel patterns of net organic carbon production and net calcification in three contrasting functional units from the Colombian Caribbean: rhodoliths, spheric free-living colonies (coraliths) of the coral *Siderastrea radians*, and colonized artificial substrates mimicking the rhodolith shape. In situ incubations were conducted during morning, afternoon, and nighttime periods under natural environmental conditions. Significant diel variation was observed across all functional units, with higher daytime net organic carbon production and calcification and reduced or negative nighttime values. Rhodoliths exhibited the highest daytime metabolic rates and the strongest diel variability, whereas corals showed comparatively lower but more stable metabolic patterns across light and dark conditions. Colonized artificial substrates displayed intermediate metabolic rates but pronounced proportional diel shifts, including consistent nighttime net $CaCO_3$ dissolution. Morning-to-night metabolic ratios revealed marked differences among functional units in the balance between daytime net organic carbon production and nighttime respiratory losses, as well as between light and dark calcification. Comparisons between daytime net organic carbon production and light calcification further indicated contrasting metabolic allocation patterns among systems. Corals exhibited proportionally higher net organic carbon production relative to calcification than rhodoliths and colonized artificial substrates. These findings demonstrate that calcifying benthic systems differ not only in metabolic magnitude but also in the temporal expression of organic and inorganic carbon processes. In addition, the affordable and highly scalable artificial substrate may eventually contribute to reef metabolism and conservation. The results suggest that biological organization and substrate identity may influence fine-scale carbonate chemistry variability in shallow tropical ecosystems, with implications for understanding benthic carbon cycling and the ecological functioning of natural and artificial reef-associated habitats.

1. Introduction

Human-induced CO_2 emissions have increased, owing to the rise in fossil fuel consumption since the Industrial Revolution in the 18th century (Leung, Zhang & Connell, 2022). The oceans serve as a significant sink for anthropogenic CO_2, absorbing approximately 48% of these emissions since the onset of the Industrial Era (Sabine et al., 2004). When atmospheric CO_2 reacts with seawater, it forms carbonic acid (H_2CO_3). This compound then dissociates into bicarbonate (HCO_3^-) and carbonate (CO_3^{2-}), releasing hydrogen ions (H^+) (Leung, Zhang & Connell, 2022). While the ocean's absorption of CO_2 mitigates the accumulation of greenhouse gases and increasing temperatures in the Earth's atmosphere, it causes ocean acidification (OA). This process alters the carbonate chemistry of the ocean, decreasing the pH and the saturation states of calcium carbonate ($CaCO_3$) such as aragonite and calcite, which are essential for marine calcifying organisms within coral reef ecosystems (Doney et al., 2009).

There is high confidence that organisms forming calcareous structures exhibit greater susceptibility to ocean acidification compared to non-calcifying species (Cooley et al., 2022). Ocean acidification imposes a twofold threat to reef calcifiers such as scleractinian corals and crustose coralline algae (CCA): it not only diminishes the ability of organisms to calcify but also accelerates the dissolution of their calcium carbonate ($CaCO_3$) structures (Kleypas et al., 2006; Cooley et al., 2022). The rapid pace of this change produces significant concern, as many marine calcifiers may struggle to adapt quickly enough (Guinotte & Fabry, 2008; Cooley et al., 2022). The management of CO_2 in marine ecosystems increasingly considers nature-based solutions aimed at long-term carbon storage (Macreadie et al., 2021). In this context, photosynthetic calcifying organisms such as corals and rhodoliths have been recognized for their role in the sequestration of carbon at ecosystem scales through the production and accumulation of $CaCO_3$ (Amado-Filho et al., 2012; Cornwall et al., 2023; Schubert et al., 2024). Although $CaCO_3$ precipitation is associated with CO_2 release in seawater, it simultaneously contributes to the long-term carbon storage when carbonate structures are preserved and buried. Thus, these organisms play a key role in maintaining carbonate budgets and sustaining carbon storage in benthic ecosystems over extended timescales (Costa et al., 2023; Tuya et al., 2023).

Calcifying benthic phototrophs play a central role in shallow marine carbon cycling through the tightly coupled processes of photosynthesis-respiration and calcification-dissolution (Gattuso, Allemand & Frakingnoulle, 1999; Cohen, Dubinsky & Erez, 2016). The relationship between photosynthesis and calcification links organic and inorganic carbon dynamics and has been widely observed across calcifying communities (Gattuso, Pichon & Frankignoulle, 1995; Suzuki, Nakamori & Kayanne, 1995). However, a detailed mechanistic understanding at the organismal scale remains limited (Borowitzka & Larkum, 1987; McCoy et al., 2023; Mao, Burdett & Kamenos, 2024). Accordingly, metabolic coupling is here defined as the degree to which daytime net organic carbon production offsets nighttime respiratory losses, and daytime calcification offsets nighttime dissolution within each functional unit. This metric is used descriptively to compare the relative balance between opposing metabolic processes under diel conditions, without inferring causal or mechanistic relationships.

In photosynthetic calcifiers such as scleractinian corals and rhodoliths, metabolism is inherently dynamic and strongly structured by diel light cycles. Numerous studies have demonstrated that calcification rates can be influenced by both photosynthetically enhanced calcification, which depends on energy produced during photosynthesis and associated pH changes at the algal surface, and by light-enhanced calcification (LEC), a process independent of photosynthesis that relies on light-mediated physiological processes to elevate surface pH and promote calcification (Jokiel, Jury & Rodgers, 2014; Hofmann, Koch & Beer, 2016; Cyronak et al., 2018; McNicholl, Koch & Hofmann, 2019; Mallon et al., 2022; Mao, Burdett & Kamenos, 2024). In corals, while endosymbiotic Symbiodinaceae algae stimulate calcification through photosynthetic CO_2 uptake and consequent pH elevation in the calcifying medium, light can also directly enhance calcification via host-controlled mechanisms (Furla et al., 2000; Gorbunov & Falkowski, 2002; Levy et al., 2007; Cohen, Dubinsky & Erez, 2016). Similarly, crustose coralline algae, including rhodoliths-forming species, employ light-driven but photosynthesis-independent mechanisms

associated with processes such as proton pumping and ion regulation which likely influence surface pH and local carbonate chemistry (Hofmann, Koch & Beer, 2016; Hofmann, Schoenrock & de Beer, 2018; McNicholl, Koch & Hofmann, 2019). In this context, calcification in coralline algae and corals may occur during both day and night periods (Allemand et al., 2011; Jokiel, Jury & Rodgers, 2014; McCoy et al., 2023). However, night calcification in corals and coralline algae is highly variable with the majority of species showing negative rates (net $CaCO_3$ dissolution) in darkness (Sordo et al., 2018; Venn et al., 2019; Ross et al., 2022; Schmidt et al., 2022; Schubert et al., 2024). These findings highlight the importance of considering species-specific responses and environmental conditions when evaluating the diel dynamics of calcification in these organisms. Because calcification and metabolic response underpin the structural integrity and persistence of reef habitats, understanding how different benthic components regulate diel carbon dynamics is essential for predicting their contribution to reef resilience under environmental change, particularly in the context of ocean acidification and habitat degradation.

Metabolic processes influence the exchange of inorganic carbon between calcifying phototrophs and the surrounding seawater, thereby modifying local carbonate chemistry through changes in dissolved inorganic carbon (DIC), total alkalinity (TA), and hydrogen ion concentration (Suzuki, Nakamori & Kayanne, 1995; Gattuso, Allemand & Frakingnoulle, 1999; Albright et al., 2015). Photosynthesis and respiration primarily control DIC and pH by mediating CO_2 uptake and release, while net photosynthesis reflects the balance between these opposing processes without directly altering TA. In contrast, net calcification integrates $CaCO_3$ precipitation and dissolution and directly modifies TA. Together, these integrated metabolic processes contribute to short-term changes in carbonate chemistry, producing diel fluctuations in DIC and TA (Jokiel, Jury & Rodgers, 2014; Cyronak et al., 2018). These organism-level metabolic processes provide a framework for examining how biological activity modulates local seawater carbonate chemistry, enabling direct comparisons between naturally occurring calcifying organisms and biologically colonized substrates under shared environmental conditions.

In addition to natural free-living calcifying organisms, this study also considers artificial spherical substrates designed to promote the colonization of marine phototrophs and calcifying organisms (e.g., filamentous algae and crustose coralline algae). After eight months of in situ deployment, these substrates supported naturally developed benthic assemblages capable of sustaining biologically mediated processes such as photosynthesis and $CaCO_3$ precipitation, potentially influencing surrounding seawater carbonate chemistry. Evaluating these systems provides an opportunity to examine how biologically colonized artificial structures contribute to carbon dynamics in shallow marine environments and to compare their emergent metabolic properties with those of physiologically integrated calcifying organisms such as rhodoliths and corals.

Recent perspectives on the future of tropical reefs suggest that shifts in benthic community composition driven by climate change may increase the relative importance of alternative calcifying organisms, including coralline algae and rhodolith-forming species, in sustaining carbonate production and ecosystem functioning (Sánchez et al., 2025). Although the future contribution of these organisms remains uncertain, understanding how their metabolic performance compares with that of corals under

natural conditions is important for evaluating their potential functional role in future reef scenarios. In this context, quantifying diel organic and inorganic carbon dynamics across different calcifying systems can provide insight into the diversity of metabolic strategies that contribute to carbonate cycling in tropical coastal ecosystems.

The aim of this study was to quantify and compare patterns of organic and inorganic carbon dynamics across daylight and nighttime periods among functional units representing different levels of biological organization, including organism-level systems (free-living corals or coraliths and rhodoliths) and structure-level systems (colonized artificial substrates), under natural light conditions. We hypothesize that *Siderastrea radians* coraliths, rhodoliths, and colonized artificial substrates differ in the relative balance between organic and inorganic carbon processes, reflecting contrasts in biological organization. In rhodoliths, both photosynthesis and calcification occur within the epithallial layer in direct contact with the surrounding seawater, whereas in corals, photosynthesis is mediated by symbiotic zooxanthellae and calcification occurs in the subcalicoblastic space, which is partially isolated from the external environment by coral tissue. In contrast, colonized artificial substrates represent structure-level systems in which metabolic signals may emerge from mixed assemblages of organisms growing on the substrate surface, rather than from a single, integrated physiological unit. Based on these differences, rhodoliths may exhibit more direct and temporally responsive metabolic patterns to changes in light availability, corals may display comparatively less temporally variable responses, and artificial substrates may show more variable and less coordinated patterns reflecting the composite nature of the associated community. As a result, we expect these systems to differ not only in the relative balance between organic and inorganic carbon processes, but also in the variability and temporal expression of these processes under natural light conditions, with implications for their functional roles in organism- and structure-level carbon dynamics

2. Methods

From January 8th to 13th – 2024, we manually collected rhodoliths (sensu Jardim et al., 2025) (Fig. 1D) from a fringing reef on the northern side of Isla Grande (10.1836 N, -75.7436 W) and free-living spherical colonies of *Siderastrea radians* coral or coraliths (Fig. 1F) from a seagrass environment on the southern side of Isla Grande (10.1714 N, -75.746 W), between 2 and 4 meters depth (Figure S1 supplementary material). Isla Grande is part of the marine protected area within the Corales del Rosario and San Bernardo National Natural Park, located in the archipelago of the Rosario Islands, Cartagena, Colombian Caribbean. Artificial substrates (Fig. 1B) consisted of spherical units of expanded clay used as settlement surfaces for marine phototrophs and calcifying organism. These substrates were installed eight months prior to the experiment in a sandy area within a coral reef and were allowed to undergo natural colonization under ambient environmental conditions before the experimental incubations.

Experimental deployment

We conducted in situ experiments with each functional unit type (corals, rhodoliths, and colonized artificial substrates) using custom-made acrylic incubation chambers (volume ~ 800 mL) (Fig. 1A, C, E, and F) following the methodology used by Gómez et al (2023). All substrates were incubated under identical conditions, including experimental design, deployment depth, and incubation duration.

The incubation chambers were deployed at a depth of 3 m (Fig. 1A) and secured to polyvinyl plastic quadrants (50 × 50 cm), which were ~70 cm above the substrate in the water column. Positive buoyancy was achieved using polystyrene floats attached to the sides of the structure. Each corner of the quadrant was anchored to the substrate with a plastic chain connected to a lead weight, minimizing displacement while allowing movement in response to prevailing currents. This configuration promoted natural water circulation within the chambers, ensuring uniform distribution of dissolved constituents (Hurd, 2000). The study site was characterized by a sandy bottom with scattered gravel deposits, located at the ecotone between a seagrass meadow and a patch coral reef. Hydrodynamic conditions during the sampling period were predominantly unidirectional, with water flow generally moving from the coral reef toward the seagrass meadow.

Photosynthetically Active Radiation (PAR) (µmol photons m^{-2} s^{-1}) was measured close to the incubation set-up, with an Odyssey® data logger, which recorded PAR at 10 seconds intervals throughout each incubation period (morning and afternoon) for each functional unit. The sensor was positioned vertically to capture measurements of PAR within the 400–700 nm wavelength range. Prior to deployment, the Odyssey® PAR logger was calibrated against a Li-Cor Quantum Sensor LI-190 to convert recorded pulses into µmol photons m^{-2} s^{-1}.

To evaluate organic and inorganic metabolic rates (photosynthesis-respiration, calcification-dissolution) we conducted incubations separately for each functional unit type, at three times of the day: morning between 9:00–12:00, afternoon between 14:30–17:00, and night between 19:00–22:00. Five replicate units (n = 5) of each functional unit type (corals, rhodoliths, and colonized artificial substrates) were incubated individually using acrylic chambers for two hours per session (Fig. 1). The same individual corals, rhodoliths, and colonized artificial substrates were used across all incubation periods. Between incubations, specimens were kept in translucent mesh enclosures, each labeled with the corresponding chamber number to maintain a consistent match between organism and chamber across all sessions. To account for changes in the metabolic activity associated with background microbial activity, a blank chamber containing only seawater was incubated concurrently under the same conditions. This value was then subtracted from the value of the chamber containing the specimens (Figueiredo et al., 2012). We collected an in situ seawater sample at the time of closing the chambers, which serve as the initial time (T_1) measurement for the physicochemical variables. Care was taken at the time of collection to ensure no bubbles were left inside the container before closing (Dickson, Sabine & Christian, 2007). At the start and end of each incubation trial we measured temperature, salinity, dissolved oxygen and pH_T (total scale) in the initial seawater sample and in each of the chambers at the end of the incubation period to get the difference (Δ values) in metabolic rates. Salinity was taken with a handheld refractometer (Vital SineTM, resolution 1ppt), dissolved oxygen and temperature was taken with a RDO

Thermo Scientific Orion Star A223 (resolution 0.01 mg L-1, accuracy ± 0.2%; temperature resolution 0.1°C, accuracy ± 0.1°C), and pH was taken in mV (millivolts) with a pH/temp probe Thermo Scientific Orion Star A121 (resolution 0.1mV, accuracy ± 0.2mV, temperature resolution 0.1°C, accuracy ± 0.1°C) immediately after collection. For pH_T, we used a glass electrode (ROSS Ultra pH/ATC Triode 8107BNUMD) that was contrasted with a Certified Reference Tris–HCL buffer solution (Dickson Lab., Scripps Institution of Oceanography, USA). Additionally, in-situ temperature was monitored with a HOBO® sensor (Onset®) pendant UA-002 throughout the duration of the trials (precision 0.14°C, accuracy ± 0.53°C). All seawater samples were collected in 250 mL clean high-density polypropylene plastic bottle container and preserved with 100 µL of saturated mercury chloride solution ($HgCl_2$) to avert alterations in the carbonate chemistry resulting from biological activity (Dickson, Sabine & Christian, 2007; Mos et al., 2021). The containers were stored at room temperature until analysis, which was performed within two months of collection.

Laboratory analysis

We employed the alkalinity anomaly method to calculate the calcification-$CaCO_3$ dissolution rates (Chisholm & Gattuso, 1991). Total alkalinity (TA) was determined by open cell potentiometric titration using a Metrohm Titrino Plus 877 following standard protocols (Dickson, Sabine & Christian, 2007) (SOP3) using hydrochloric acid as titrant (0.1 mol L^{-1} HCl buffered in 0.6 mol L^{-1} NaCl, Batch A26 CRM Dickson Lab, Scripps Institution of Oceanography, USA). The carbonate system was derived from total alkalinity (TA) and pH_T using the Excel-CO2SYS program (Pierrot et al., 2006), taking as parameters the dissociation constant for carbonic K1 and K2 from Mehrbach et al., (1973), refit by (Dickson & Millero, 1987), $KHSO_4$ by (Dickson, 1990) and Boron by (Lee et al., 2000). These two parameters were taken as input alongside with temperature and salinity data to characterize DIC (µmol kg^{-1}), partial pressure of CO_2 in the system (µatm pCO_2), bicarbonate (HCO_3^-) (µmol kg^{-1}), carbonate concentration (CO_3^{2-}) (µmol kg^{-1}) and aragonite and calcite saturation states (Ω_{arag} and $\Omega_{calcite}$). To determine the accuracy of the analysis, the samples were validated with certified reference material (CRM) for TA, which were < 0.5% estimated error (TA: ±10 µmol kg^{-1} SW) (Batch 139, CRM Dickson Lab, Scripps Institution of Oceanography, USA).

Quantification of metabolic rates

Net organic carbon production (µmol C cm^{-2} h^{-1}) by each functional unit during light and dark incubations was estimated from changes in dissolved oxygen (DO) concentrations, assuming that one mole of carbon is fixed for every mole of O_2 produced via photosynthesis (Jokiel, Jury & Rodgers, 2014) and that one mole of CO_2 is produced for every mole of O_2 consumed by respiration. These estimates correspond to net organic carbon production (P_{DO}), as they reflect the balance between photosynthetic oxygen evolution and concurrent respiratory oxygen consumption during light incubations, and therefore do not represent gross photosynthetic rates. Changes in DO were calculated by subtracting the initial DO

concentration from the final value at the end of each incubation period (ΔDO = final – initial). The calculation was performed using the following equation:

$$P_{DO} = \frac{\Delta DO \times V}{SA \times t}$$

where ΔDO indicates the variations in DO concentrations in μmol L^{-1} of seawater, *V* is the chamber volume in liters (calculated as the total chamber volume minus the volume of the specimen, the latter determined by the water displacement technique), *SA* represents the functional unit surface area (cm^2), and *t* refers to the incubation time in hours. Negative values of P_{DO} occur when oxygen consumption by respiration exceeds oxygen production by photosynthesis, typically under dark incubation conditions.

Net calcification (G_{net}) (μmol $CaCO_3$ cm^{-2} h^{-1}) under both light and dark incubation conditions was determined using the alkalinity anomaly method, as described by the following equation:

$$G_{net} = \frac{(-\frac{\Delta TA}{2}) \times V}{SA \times t}$$

where ΔTA denotes the changes in total alkalinity (TA) concentrations in μmol kg^{-1}, *V* is the volume of the incubation chamber in liters (calculated as for P_{DO}), *SA* is the surface area of the specimen, and *t* is the time in hours. The change in total alkalinity (ΔTA) is divided by 2, considering that each mole of $CaCO_3$ precipitated or dissolved corresponds to a change of two moles in TA (Chisholm & Gattuso, 1991).

To normalize the results from each incubation, the surface area of each sphere was calculated using the Polycam - LiDAR & 3D Scanner application for iPhone and Android. Because the organisms were incubated in transparent acrylic chambers suspended 70 cm from the bottom that allowed light to reach their entire surface, we generated 3D images capturing the complete semispherical surface of each functional unit. 3D image files in .glb format were obtained and subsequently analyzed with Blender 4.1 software to calibrate the size and calculate the total surface area of each specimen. For artificial substrates, surface area calculations focused on the externally exposed and colonized surface, without partitioning surface area among colonizing biological groups. Three-dimensional models captured the full spherical geometry, and areas lacking visible biological colonization were excluded from surface area estimates to ensure that metabolic rates reflected biologically active surfaces only.

To characterize the temporal dynamics of metabolic activity in the studied functional units, we first conducted a broad assessment of net organic carbon production and net calcification at three distinct time points: morning, afternoon, and night. This initial exploration allowed us to observe how metabolic rates responded to natural variations in irradiance throughout the day. Based on this assessment, we identified the light and dark periods as those showing the clearest physiological contrasts: the daytime period was characterized by maximum light availability and enhanced carbon uptake, while nighttime conditions reflected the absence of light and a shift toward respiratory processes and net calcification or

dissolution. Consequently, subsequent analyses focused on comparing these two periods to quantify net daily balances of organic (daytime net organic carbon production vs. nighttime respiratory carbon loss) and inorganic (daytime vs. nighttime calcification) carbon dynamics. This approach allowed for a more robust and integrative evaluation of the organismal or structure contributions to carbon cycling within a simplified light-to-dark framework.

To better characterize the diel metabolic balance of the studied models, we calculated the metabolic coupling as absolute ratios between light and dark periods. This approach emphasizes the relative magnitude of daytime net organic carbon production by photosynthesis vs. nighttime respiratory carbon loss, as well as the light vs. dark calcification, independently of process directionality. By focusing on the intensity of these processes rather than their sign, these ratios offer a useful proxy for assessing the extent to which daytime metabolic activity (photosynthesis or calcification) compensates for nighttime losses (respiration or dissolution). Values greater than one suggest a net positive contribution to organic or inorganic carbon stocks over a morning-to-night comparison, whereas values near or below one indicate metabolic compensation or net carbon loss.

Additionally, we included the non-absolute ratio between net organic carbon production and net calcification (P_{DO}/G_{net}) during the daytime period of maximum physiological contrast with nighttime conditions to explore the functional relationship between these two light-dependent processes. This approach provided a comparative framework to assess whether carbon uptake is preferentially directed toward net organic carbon production or net inorganic $CaCO_3$ precipitation. This metric offers insights into metabolic allocation patterns and potential roles of each functional unit in organism- and structure-level carbon dynamics under natural diel conditions.

Statistical analysis

A repeated measures Analysis of Variance (ANOVA) was conducted using the afex package (version 1.4.1) (Singmann et al., 2024) to assess the effects of time of day (morning, afternoon, night) and type of functional unit (coral, rhodolith, or colonized artificial substrate) on the rates of photosynthesis and respiration estimated from dissolved oxygen changes (P_{DO}) and light and dark net calcification (G_{net}) as dependent variables. Each subject (individual functional unit) was measured at all three times of day. The sphericity assumption for the within-subject factor (time of day) and its interaction with functional unit type was tested using Mauchly's test. As the assumption was violated, the Greenhouse-Geisser correction was applied to adjust the degrees of freedom. Homogeneity of variances across combinations of functional unit type and time of day was assessed using Levene's test, and normality of residuals was evaluated with the Shapiro–Wilk test, confirming that all other assumptions were satisfactorily met. When significant interaction effects were detected in the ANOVA, post hoc pairwise comparisons were conducted using estimated marginal means (Emmeans) using the package emmeans (version 1.11.0) (Lenth et al., 2025) with Bonferroni adjustment to account for multiple testing and identify differences between combinations of functional unit type and time of day. All the statistical

analysis and figures were performed in RStudio (version R. 4.4.3), with data visualization in the ggplot2 package (version 3.5.1) (Wickham, 2016).

3. Results

3.1. Metabolic rates across different times of the day

Net organic carbon production rates, estimated from changes in dissolved oxygen (P_{DO}), varied markedly throughout the diel cycle and differed among functional units, with their magnitude shifting over the course of the day. A significant interaction between time and functional units was observed ($F_{4, 24}$ = 11.03, $p < 0.001$, ges = 0.52) (Table S1). During daylight periods, net organic carbon production was positive in all groups. In the morning, rhodoliths exhibited significantly higher P_{DO} rates than both artificial substrates (difference = 0.228 μmol C cm^{-2} h^{-1}, ≈ 23.4% higher, p = 0.0472) and corals (difference = 0.289 μmol C cm^{-2} h^{-1}, ≈ 42.1% higher, p = 0.0105) (Table S2, Fig. 2B). In contrast, no significant differences were detected between artificial substrates and corals (p = 0.7830). During the afternoon, differences among functional units became more pronounced. Rhodoliths exhibited significantly higher P_{DO} rates than both artificial substrates (difference = 0.668 μmol C cm^{-2} h^{-1}, ≈ 72.1% higher, $p < 0.0001$) and corals (difference = 0.465 μmol C cm^{-2} h^{-1}, ≈ 101% higher, p = 0.0001). No significant differences were detected between artificial substrates and corals (p = 0.0836), although artificial substrates tended to show lower values. In contrast to daytime conditions, no significant differences in net organic carbon production were detected among functional units at night (all $p > 0.05$) (Table S2). Although artificial substrates tended to exhibit slightly higher (i.e., less negative) values compared to rhodoliths and corals, these differences were not statistically significant (Fig. 2B).

G_{net} also varied across the diel cycle (Table S1) with interaction between both factors recorded ($F_{4, 24}$ = 5.02, p = 0.004, ges = 0.37). Net $CaCO_3$ production was positive during daylight hours and decreased at night across all functional units (Fig. 2A). In the morning, rhodoliths exhibited significantly higher G_{net} than corals (difference = 0.132 μmol $CaCO_3$ cm^{-2} h^{-1}, ≈ 118% higher, p = 0.0119), whereas artificial substrates did not differ significantly from either rhodoliths (p = 0.1399) or corals (p = 0.4856) (Table S2). During the afternoon, rhodoliths showed significantly higher net production than both artificial substrates (difference = 0.244 μmol $CaCO_3$ cm^{-2} h^{-1},$^{-1}$,≈ 79.5% higher, $p < 0.0001$) and corals (difference = 0.173 μmol $CaCO_3$ cm^{-2} h^{-1}, ≈ 129% higher, p = 0.0011), while no significant differences were detected between artificial substrates and corals (p = 0.2292). In contrast, no significant differences were observed among functional units at night (all $p > 0.05$), with relatively small pairwise differences (|difference estimate| ≤ 0.094 μmol $CaCO_3$ cm^{-2} h^{-1}) (Fig. 2A; Table S2).

These metabolic patterns were closely associated with irradiance levels during the incubations. Photosynthetically active radiation (PAR) averaged 1,276 ± 532 μmol photons m^{-2} s^{-1} in the morning and declined to 465 ± 240 μmol photons m^{-2} s^{-1} in the afternoon. This reduction in light availability paralleled the decrease in both net organic carbon production (P_{DO}) and net calcification (G_{net}) observed later in the

day, reinforcing the strong light dependence of these processes. Based on these irradiance conditions and the consistently higher metabolic rates recorded across functional units, morning measurements were considered the most representative of peak daytime performance. Accordingly, morning values provide a consistent reference for comparisons with nighttime metabolic rates and for assessing differences between daytime and nighttime metabolic rates in rhodoliths, corals, and colonized artificial substrates.

3.2 Net metabolic balance in morning – night comparisons:

The values shown in Table 1 and Fig. 3 collectively show the morning-to-night ratios of P_{DO} and G_{net} rates for rhodoliths, corals, and colonized artificial substrates, highlighting both absolute values (|morning/night| ratios) and non-absolute (P_{DO}/G_{net} light ratio) relationships in each functional unit type.

P_{DO} was highest in rhodoliths during the morning (0.976 ± 0.2 µmol C cm^{-2} h^{-1}), followed by colonized artificial substrates (0.747 ± 0.1 µmol C cm^{-2} h^{-1}) and corals (0.686 ± 0.1 µmol C cm^{-2} h^{-1}). At night, all functional units shifted to negative P_{DO} values, indicating net organic carbon loss (Fig. 3B, Table 1). However, despite these differences in morning P_{DO}, absolute diel variation followed a contrasting pattern. Colonized artificial substrates exhibited the highest |morning/night| ratio between daytime net organic carbon production and nighttime respiratory carbon loss (P_{DO} |morning/night| ratio = 5.37), exceeding that of rhodoliths (3.83) and corals (2.06) (Table 1). Rhodoliths showed an intermediate ratio, whereas corals displayed the lowest proportional variation, indicating a comparatively smaller difference between daytime and nighttime P_{DO}. In all cases, P_{DO} ratios remained above 1, indicating higher daytime net organic carbon production relative to nighttime respiratory losses, resulting in a positive net organic carbon balance over the morning-to-night comparison.

During the morning period, all functional units exhibited positive net calcification. Morning calcification rates were highest in rhodoliths (0.244 ± 0.1 µmol $CaCO_3$ cm^{-2} h^{-1}), followed by colonized artificial substrates (0.161 ± 0.04 µmol $CaCO_3$ cm^{-2} h^{-1}) and corals (0.112 ± 0.1 µmol $CaCO_3$ cm^{-2} h^{-1}) (Fig. 3A, Table 1). At night, there were clear differences among groups. Nocturnal calcification in corals remained positive on average (0.070 ± 0.1 µmol $CaCO_3$ cm^{-2} h^{-1}), although individual values showed substantial variability, with some approaching zero (Table 1 and Fig. 3A). In contrast, rhodolith calcification decreased at night (0.021 ± 0.1 µmol $CaCO_3$ cm^{-2} h^{-1}), with one negative value. Colonized artificial substrates exhibited negative nocturnal G_{net} values on average (– 0.0228 ± 0.01 µmol $CaCO_3$ cm^{-2} h^{-1}). However, when expressed as morning-to-night ratios, differences among groups increased. Rhodoliths exhibited the highest morning-to-night G_{net} ratio (11.6), followed by colonized artificial substrates (7.06) and corals (1.58).

Table 1
Absolute and non-absolute ratios in *S. radians* corals, rhodoliths and colonized artificial substrates: Mean ± standard deviations (SD) of net organic carbon production rates (P_{DO}) expressed in µmol C cm^{-2} h^{-1}, and net calcification rates (G_{net}) expressed in µmol $CaCO_3$ cm^{-2} h^{-1} during morning and night periods. Rate ratios were calculated for both morning and night periods (|morning / night|), to P_{DO} (daytime-to-nighttime net organic carbon production rate ratio) and G_{net} (light-to-dark calcification rate ratio), and the light P_{DO}/G_{net} ratio (photosynthesis-to-calcification rate ratio).

		P_{DO}	G_{net}	|morning / night| ratios		light ratio
Functional unit	Time of the day	Mean (± SD)	Mean (± SD)	P_{DO}	G_{net}	P_{DO} / G_{net}
Rhodoliths	morning	0.976 (± 0.2)	0.244 (± 0.1)	3.83	11.6	4.0
	night	-0.255 (± 0.0)	0.021 (± 0.1)			
Corals	morning	0.686 (± 0.1)	0.112 (± 0.1)	2.06	1.58	6.13
	night	-0.334 (± 0.1)	0.070 (± 0.1)			
Artificial	morning	0.747 (± 0.1)	0.161 (± 0.04)	5.37	7.06	4.64
	night	-0.139 (± 0.02)	-0.0228 (± 0.01)			

The P_{DO}/G_{net} represents the proportional relationship between net organic carbon production and net calcification under light conditions (Fig. 3C, Table 1). In all functional units, P_{DO} exceeded G_{net} during the morning, with ratios above 1 in all cases. However, ratio values differed among groups, where corals exhibited the highest P_{DO}/G_{net} ratio (6.13), indicating that P_{DO} was more than six times higher than G_{net} under light conditions. Colonized artificial substrates displayed an intermediate ratio (4.64), while rhodoliths showed the lowest P_{DO}/G_{net} ratio (4.0). Although rhodoliths exhibited the highest rates of both P_{DO} and G_{net}, they had lower P_{DO}/G_{net} ratios relative to the other functional units.

4. Discussion

4.1 Overview of diel carbon dynamics across functional units

This study presents an in situ comparative analysis of organism- and structure-level carbon dynamics in shallow tropical systems by quantifying organic (daytime net organic carbon production vs. nighttime respiratory carbon loss) and inorganic (daytime vs. nighttime net calcification) processes in rhodoliths, *Siderastrea radians* coraliths, and biologically colonized artificial substrates. Our results indicate that these functional units exhibit distinct metabolic patterns that are associated with differences in net

organic carbon production and $CaCO_3$ precipitation rates, as well as contrasting diel amplitudes and functional relationships between net organic carbon production (P_{DO}) and calcification (G_{net}), indicating a possible contribution to short-term variability in seawater carbonate chemistry. Rhodoliths exhibited strong light-related increases in metabolic rates and pronounced morning-to-night ratio variability, corals displayed comparatively lower but more stable rates across the diel cycle, and colonized artificial substrates showed intermediate rates with high proportional diel contrasts. Together, these organism- and structure-level patterns underscore the functional heterogeneity of benthic calcifiers and provide initial baseline information to contextualize their role in short-term carbonate chemistry dynamics in tropical coral reef and seagrass-associated systems. These differences may be relevant for reef conservation, as shifts in benthic community composition could be associated with changes in local carbonate chemistry dynamics under changing environmental conditions.

4.2 Diel patterns in net organic carbon production (P_{DO})

Net P_{DO} exhibited marked diel variability and clear differences among functional units, shaping short-term carbon dynamics. During daylight, rhodoliths consistently showed higher P_{DO} rates than both corals and colonized artificial substrates, with these differences becoming more pronounced under higher irradiance. In the morning, rhodolith P_{DO} was approximately 42% higher than in corals and 23% higher than in artificial substrates, whereas no significant differences were detected between corals and artificial substrates. During the afternoon, rhodoliths exhibited substantially higher P_{DO} rates than both corals (≈ 101% higher) and artificial substrates (≈ 72% higher), again with no significant differences between corals and artificial substrates. These patterns are consistent with the light dependence of net organic carbon production and its association with photosynthetic activity under daylight conditions (Larkum, Grossman & Raven, 2020). P_{DO} values became negative at night across all functional units, consistent with net respiratory carbon loss under dark conditions. No significant differences were detected among rhodoliths, corals, and artificial substrates during nighttime incubations. These results are consistent with diel patterns observed for rhodoliths and corals across tropical and subtropical systems (Kamenos et al., 2013; Martin et al., 2013; Noisette et al., 2013a, 2013b; Jokiel, Jury & Rodgers, 2014; Gutner-Hoch et al., 2016; Hofmann, Koch & Beer, 2016; Sordo et al., 2018; Carvalho et al., 2020; Schubert et al., 2021; MacDonald et al., 2025).

The consistently higher daytime P_{DO} observed in rhodoliths indicates higher contribution to short-term CO_2 uptake under high irradiance conditions relative to corals and colonized artificial substrates. Collectively, these patterns highlight functional differences among calcifying organisms and structures in their association with seawater carbonate chemistry dynamics. Interestingly, these findings contrast with studies reporting lower photosynthetic rates in crustose coralline algae (CCA) compared to massive corals under controlled experimental conditions (Mallon et al., 2022). This discrepancy may be related to differences in species identity and growth form, particularly between free-living rhodoliths and attached crustose CCA, as well as to differences in experimental design (e.g., incubation protocols, light regimes, and water chemistry). The heterogeneous morphology of crustose coralline algae may create

microenvironmental conditions that influence local chemical gradients; for example, structural complexity has been linked to thicker diffusive boundary layers (DBL) and localized pH elevation under light exposure, processes that have been associated with enhanced net organic carbon production and calcification rates (Cornwall et al., 2014; Schubert et al., 2021).

In rhodoliths, the intermediate daytime-to-nighttime of P_{DO} ratio (3.83) indicates an imbalance between daytime net organic carbon production and nighttime respiratory losses. This pattern, in which daytime carbon fixation markedly exceeds nocturnal respiration, has also been reported in temperate rhodolith beds exhibiting positive net carbon balances across diel cycles (Sordo et al., 2020). Previous studies have shown that photosynthetic performance in rhodoliths can vary with local light regimes, with both inter- and intraspecific differences in carbon fixation associated with irradiance conditions (Schubert et al., 2022). In this context, the net daytime organic carbon gain observed in rhodoliths in the present study is consistent with patterns reported for rhodolith-forming species under favorable light conditions.

In contrast, *Siderastrea radians* coraliths showed a more stable daytime-to-nighttime P_{DO} ratio, with daytime net organic carbon production approximately twice nighttime respiratory losses. This ratio, greater than 1, is consistent with a net positive carbon balance during light periods and aligns with previous observations indicating that *S. radians* can maintain relatively favorable metabolic ratios under sub-optimal conditions (Lirman & Manzello, 2009). This pattern suggests a relatively stable relationship between photosynthesis and respiration, consistent with limited diel variability in metabolic rates under fluctuating environmental conditions. Daytime carbon fixation by symbiotic zooxanthellae corals exceeded nocturnal respiratory losses, a pattern consistent with previous studies showing that coral photosynthesis generally surpasses respiration during daylight hours (Gattuso, Allemand & Frankignoulle, 1999). Similar patterns have been reported in other zooxanthellate coral species exhibiting high photosynthesis-to-respiration ratios (2.5 ± 0.3) (Simancas-Giraldo et al., 2021), further supported by evidence that reduced dark respiration contributes to maintaining positive daily net photosynthesis (Anthony & Hoegh-Guldberg, 2003; Cooper et al., 2010). These species-specific differences in P_{DO} ratios between rhodoliths and the more moderate ratios observed in *S. radians* coraliths suggest variation in the balance between primary production and respiratory carbon loss at the organismal level.

Interpreting photosynthesis-to-respiration relationships in corals requires caution, as respiration is not constant throughout the diel cycle and may remain elevated during daylight despite net photosynthesis exceeding respiratory demand (Kuhl et al., 1995; Gattuso, Allemand & Frankignoulle, 1999). Because the P_{DO} measurements used here represent net oxygen-based estimates, they do not resolve simultaneous oxygen production and consumption during light incubations, which may influence estimates of net metabolic balance. Consequently, the relatively stable P_{DO} patterns observed in *Siderastrea radians* should be interpreted as net metabolic responses rather than direct estimates of gross photosynthesis or respiration. Furthermore, the specimens analyzed in this study corresponded to coraliths, free-living coral colonies, a growth form that, similarly to rhodoliths, integrates metabolic processes across an entire spherical structure exposed to surrounding seawater. Despite this morphological similarity, the spatial organization of physiological processes differs substantially between both systems. In corals,

photosynthesis occurs within symbiotic tissues overlying the carbonate skeleton, whereas in rhodoliths photosynthetic and carbonate-producing tissues are directly exposed at the algal surface. These anatomical differences may influence how metabolic activity interacts with surrounding seawater conditions and responds to environmental variability, potentially contributing to the contrasting diel patterns observed between both functional units.

4.3 Diel variation in calcification dynamics

Variation in net calcification rates (G_{net}) among functional units and across the diel cycle revealed contrasting patterns between organism-level substrates and colonized artificial structures. The elevated G_{net} observed in rhodoliths relative to both artificial substrates and corals differs from patterns reported in studies dominated by encrusting coralline algae and massive corals, where corals often exhibit higher calcium carbonate production (Kuffner, Hickey & Morrison, 2013; Mallon et al., 2022). For example, Kuffner et al. 2013 reported calcification rates in *Siderastrea siderea* coraliths an order of magnitude higher than in crustose coralline algae (CCA), a pattern also observed by Mallon et al. (2022), who found higher light calcification in massive corals than in CCA under mesocosm conditions. Similarly, in temperate reefs, CCA calcification has been reported to be 2–7 times lower than that of corals (Pessarrodona, Attlan & Wernberg, 2025). However, these studies have focused not on nucleated rhodolith forming algae but on those with encrusting forms, which are characterized by a bidimensional flat surface where calcification and photosynthesis occur simultaneously. In contrast, rhodolith forming algae are complex tridimensional nodules that significantly increase the surface area in contact with seawater, potentially contributing to spatial heterogeneity in metabolic activity. Calcification rates in rhodoliths are also known to vary across species and morphologies, as demonstrated by studies reporting substantial variability among different rhodolith-forming taxa (*Phymatolithon calcareum, Lithothamnion crispatum, Melyvonnea erubescens, Lithophyllum atlanticum, Phymatolithon* sp. and *Phymatolithon lusitanicum*) (Schubert et al., 2022). Together, these factors provide a plausible context for understanding why tridimensional rhodoliths may exhibit calcification rates higher than those of corals under certain environmental conditions.

Rhodoliths exhibited more pronounced differences in calcification between light and dark conditions, with morning rates more than 11 times higher than nocturnal rates (11.6), occurring alongside elevated daytime net organic carbon production (i.e., 3.83). Strong light-to-dark variability in calcification has been reported across several rhodolith species, with G_{net} values ranging from positive to negative (dissolution). For example, *Lithothamnion corralioides* and *Lithothamnion crispatum* showed higher net calcification under light than in darkness under ambient conditions (Noisette et al., 2013a; Legrand et al., 2017), with *L. crispatum* maintaining calcification at approximately 20% of its light-exposed rate (Schubert et al., 2019). Similarly, *Phymatolithon lusitanicum* has been reported to exhibit increasing calcification rates under higher light availability, while dark conditions are often associated with net $CaCO_3$ dissolution (Sordo et al., 2018). In situ experiments further show that rhodolith beds composed of *Lithothamnion crispatum* exhibit positive net calcification under light, shifting toward net dissolution in darkness (Carvalho et al., 2020). Likewise, colonized artificial substrates exhibited a marked diel contrast

in calcification, with a light-to-dark G_{net} ratio of 7.06. Although lower than that observed in rhodoliths, this ratio indicates higher net carbonate precipitation under illuminated conditions relative to darkness. Given that these measurements integrate the activity of a heterogeneous colonizing assemblage, this pronounced diel pattern likely represents the combined metabolic contributions of organisms associated with the substrate surface, rather than calcification dynamics attributable to a single organism or functional group.

Siderastrea radians coraliths showed a relatively low light-to-dark calcification ratio (1.58), with light calcification only about 1.6 times higher than at night. Compared with values commonly reported for zooxanthellate corals, where calcification under light is often approximately threefold greater than in darkness, this value falls toward the lower end of reported responses (Gattuso, Allemand & Frankignoulle, 1999). This relatively moderate diel contrast suggests that calcification in *S. radians* remained comparatively stable across light and dark conditions under the environmental conditions evaluated here. In symbiotic corals, enhanced calcification under light conditions has been associated with photosynthetic CO_2 uptake by zooxanthellae, which can elevate pH and aragonite saturation state (Ω_{arag}) within the calcifying environment during daylight (Goreau, 1959; Gattuso, Allemand & Frankignoulle, 1999; Allemand et al., 2011). However, light-enhanced calcification may also occur independently of photosynthesis, as suggested by previous studies (Al-Horani, Al-Moghrabi & de Beer, 2003a, 2003b; Cohen, Dubinsky & Erez, 2016). Additionally, light exposure has been proposed to stimulate the transport of dissolved inorganic carbon and calcium ions (Ca^{2+}) to the calcifying medium (Furla et al., 2000).

Siderastrea radians exhibits relatively stable light-associated calcification patterns consistent with those reported for symbiotic corals. Crustose coralline algae (CCA) and rhodoliths have been reported to sustain calcification through a range of compensatory mechanisms, such as elevated pH within the surface diffusive boundary layer (DBL), carbon-concentrating mechanisms and carbonic anhydrase activity, which can reduce local H^+ concentrations and generate favorable conditions for $CaCO_3$ precipitation (McNicholl, Koch & Hofmann, 2019). Distinct anatomical and physiological compartments where calcification takes place are also mentioned as a possible difference likely influencing the relative balance between light-to-dark $CaCO_3$ precipitation and dissolution. For example, in corals, calcification in form of aragonite occurs in an isolated extracellular calcifying space beneath the tissue (Gattuso, Allemand & Frankignoulle, 1999), while rhodoliths precipitate high-magnesium calcite primarily within superficial epithallial and meristematic cells (de Carvalho et al., 2022; McCoy et al., 2023). Such processes are consistent with previous studies linking daytime photosynthesis to increased calcification rates (Goreau, 1959; Gattuso, Frankignoulle & Smith, 1999; Jokiel, Jury & Rodgers, 2014; Mallon et al., 2022).

4.4 Artificial substrates as emergent metabolic systems

Our results indicate that colonized artificial substrates can act as metabolically active surfaces rather than purely physical structures. After eight months of in situ deployment, these substrates exhibited

measurable daytime net organic carbon productivity and calcification, resulting in a positive diel balance of both organic and inorganic carbon. This suggests that the observed metabolic signal arises from the combined activity of the associated biological assemblage, although its composition was not characterized in this study. In this context, carbon dynamics can be interpreted as the net outcome of concurrent autotrophic carbon fixation and heterotrophic respiration, as well as $CaCO_3$ precipitation and dissolution processes occurring at the substrate-water interface. Despite this net positive balance, calcification on artificial substrates showed strong light dependence and negative nocturnal values, consistent with respiration-driven shifts in carbonate chemistry during darkness. The absence of photosynthetic CO_2 uptake at night likely promotes localized decreases in pH and carbonate saturation state ($\Omega_{aragonite}$ or $\Omega_{calcite}$), thereby reducing net $CaCO_3$ precipitation or promoting dissolution (Eyre et al., 2014; Cyronak et al., 2013, 2018). This result is consistent with pronounced diel variability associated with changes in irradiance, rather than indicating tightly regulated calcification processes at the organism level (Gattuso, Allemand & Frakingnoulle, 1999; Jokiel, Jury & Rodgers, 2014).

In this sense, the metabolic behavior of colonized artificial substrates may reflect the integrated activity of mixed phototrophic and heterotrophic assemblages, resulting in a dynamic carbon cycling and potentially greater variability in short-term diel carbonate chemistry dynamics (Atkinson & Cuet, 2008; Andersson & Gledhill, 2013). Carbonate production arises from the balance of concurrent biological processes associated with multiple calcifying groups, rather than being attributable to a single dominant organism (Mallela & Perry, 2007; Mallela, 2013). Such functional characteristics are consistent with previous studies showing that metabolic integration in benthic assemblages can be influenced by community composition and turnover, resulting in pronounced variability in both organic and inorganic carbon dynamics over short temporal scales (Cyronak, McMahon & Eyre, 2013; Eyre, Andersson & Cyronak, 2014; Cyronak et al., 2018), a pattern consistent with the diverse and compositionally variable benthic assemblages reported for artificial substrates (Perkol-Finkel & Benayahu, 2007). This framework may explain the intermediate calcification rates and high proportional diel variability observed in artificial substrates relative to rhodoliths and corals.

4.5 Relative balance between organic production and calcification

The relative relationship between net organic carbon production and calcification under light conditions, expressed as the P_{DO}/G_{net} ratio, provides a comparative measure of the balance between organic carbon production and carbonate precipitation. Corals exhibited a higher relative contribution of net organic carbon production per unit of $CaCO_3$ precipitated compared with colonized artificial substrates and rhodoliths (Table 1; Fig. 3C), indicating larger proportional differences between net organic carbon production and calcification under light conditions.

The high P_{DO}/G_{net} ratio in *S. radians* may reflect a greater relative contribution of photosynthesis compared to calcification. This pattern is consistent with previous work reporting substantial interspecific variability in P_{DO}/G_{net} ratio among reef-building corals (Carlot et al., 2022). In that study,

differences in these ratios were interpreted in terms of contrasting energy allocation patterns, with some species exhibiting relatively greater investment in skeletal growth and others showing comparatively higher photosynthetic contributions. Given that photosynthetically derived carbon can represent a major component of the energy supply in symbiotic corals (Wooldridge, 2010), this pattern may indicate a metabolic profile in which photosynthetic carbon fixation is proportionally high relative to calcification, while maintaining comparatively moderate calcification rates.

In rhodoliths, the association between daytime P_{DO} and G_{net} is highly species-specific and shaped by complex physiological and environmental interactions (Schubert et al., 2024). Experimental studies have shown that suppression of photosynthesis is associated with species-dependent declines in calcification rates (Schubert et al., 2022). Environmental conditions are also associated with differences in this relationship, as evidenced by differences observed among geographically distinct rhodolith beds (Qui-Minet et al., 2021). Recent work also reports contrasting patterns between photosynthetic performance and calcification across coralline algae species, with some taxa exhibiting relatively higher photosynthetic rates and others higher carbonate production (Sneed et al., 2025). Together, these findings indicate that rhodoliths do not follow a single metabolic profile but instead span a spectrum of photosynthesis-to-calcification balances, which may be relevant for understanding variability in benthic carbon dynamics.

Colonized artificial substrates exhibited an intermediate P_{DO}/G_{net} ratio relative to rhodoliths and corals, indicating a greater proportional contribution of organic carbon production relative to carbonate precipitation. In early stages, experimental substrates are colonized by microbial biofilms and diverse benthic assemblages (cyanobacteria, filamentous algae, CCA, etc), whose composition typically changes through successional stages (Mallela, Milne & Martinez-Escobar, 2017; Carreira-Flores et al., 2023; Wilking, Dillon & Rakocinski, 2023; Bracho-Villavicencio et al., 2024; Carmona-Rodríguez et al., 2024; Sajid et al., 2024; Yanovski et al., 2024; Wang et al., 2026). As succession progresses, these communities transition from microbially dominated biofilms to a phototrophic and calcifying dominated taxa, influencing benthic ecosystem functioning, contributing to carbonate cycling (Wilking, Dillon & Rakocinski, 2023; Wang et al., 2026). For example, mixed assemblages developing on dead coral substrates have been shown to exhibit high daytime net photosynthesis, in some cases exceeding that of adjacent live corals, while simultaneously promoting net carbonate precipitation under light conditions and shifting toward dissolution at night, resulting in pronounced diel variability in $CaCO_3$ dynamics (Romanó de Orte et al., 2021). Consistent with these patterns, experimental substrates have demonstrated that the majority of the carbonate production has been associated with encrusting calcifiers such as CCA, supporting the view that these metabolic dynamics can emerge as integrated properties of the colonizing community rather than organism-specific processes (Goh et al., 2021). Within this framework, the high proportional variability observed in artificial substrates in this study is consistent with the possibility that it arises from shifts in the relative contributions of phototrophic and calcifying components within the assemblage.

5. Conclusions

This study shows that patterns of co-variation between net organic carbon production and net calcification differ among rhodoliths, coraliths, and colonized artificial substrates when evaluated at the organismal or structure level. Rather than following a uniform pattern, these substrate types exhibit distinct differences in the magnitude and relationships between organic and inorganic carbon processes. In this context, rhodoliths exhibit strong increases in both carbon fixation and calcification under high irradiance, followed by marked declines in darkness, consistent with a strong influence of light availability and pronounced diel variability. *Siderastrea radians* coraliths display comparatively lower but more stable rates across the diel cycle, maintaining positive calcification at night and showing patterns consistent with lower short-term variability in response to fluctuations in irradiance. Colonized artificial substrates represent a distinct case, as their metabolic dynamics emerge from the combined activity of heterogeneous benthic assemblages associated with the substrate surface, rather than from the more physiologically integrated organization observed in corals and rhodoliths. As a result, these systems exhibited intermediate rates but high proportional diel variability. These patterns indicate that differences among substrate types are expressed not only in the magnitude of metabolic rates but also in their diel dynamic of organic and inorganic carbon processes, highlighting that substrate identity is associated with differences in short-term variability in carbonate-related processes. Although these findings are based on short-term incubations, they further suggest that variability in these relationships may be associated with fine-scale variability in carbonate chemistry dynamics in shallow marine environments.

6. Recommendations and perspectives

This study presents organism-level observations for corals and rhodoliths, and structure-level data for colonized artificial substrates, indicating that these systems exhibit distinct patterns in organic carbon production and calcification–dissolution dynamics under natural diel conditions. While these results highlight consistent differences among substrate types, their broader ecological implications should be interpreted with caution and should be considered as a first step toward characterizing the relative roles of *Siderastrea radians* coraliths and rhodoliths in benthic carbon dynamics in the Colombian Caribbean.

Future work should therefore prioritize the quantification of fully integrated diel carbon dynamics, incorporating continuous or high-frequency measurements that capture transitions between light and dark periods. Methodologically, incorporating direct estimates of respiration during light incubations would improve the interpretation of metabolic rates, as net oxygen-based measurements alone cannot resolve concurrent photosynthesis and respiration. This approach would improve estimates of the balance between photosynthetic carbon fixation and respiratory carbon loss, allowing more accurate assessment of net organic and inorganic carbon budgets over complete daily cycles.

Building on the contrasts observed among substrate types, further research should expand this comparative framework across taxa and structural forms. Addressing these differences would benefit

from improved taxonomic resolution and cross-habitat comparisons, as rhodoliths exhibit substantial inter- and intra-specific variability in calcification and photosynthetic rates, and coral species differ in skeletal architecture and physiological response. Extending this approach to multiple species within each group will help determine whether the patterns reported here reflect generalizable functional traits or species-specific responses.

For colonized artificial substrates, future studies should aim to characterize the taxonomic and functional composition of the colonizing assemblages, as the metabolic signals measured here represent emergent properties of mixed communities rather than organism-specific processes. Linking metabolic rates with community composition will be important for understanding the drivers of the diel variability observed in these structures.

Finally, bridging organism- and structure-level measurements with community- and ecosystem-scale assessments remains an important challenge. Integrating experimental incubations with approaches such as benthic chamber deployments, spatial surveys, or modeling frameworks would help assess how substrate-specific metabolic functioning scales to reef-scale carbon cycling and carbonate chemistry under natural environmental variability.

Declarations

7. Ethics and Integrity statements:

Data Availability Statement: Data available in a publicly accessible repository DOI: https://doi.org/10.6084/m9.figshare.27628080.v1

Ethics and permit approval statement: No ethical approval was required.

Funding statement: This research was funded by Universidad de los Andes through the project INV-2022-151-2609 and Minciencias program "Observatorio de la microbioerosión, acidificación oceánica y la disolución en arrecifes coralinos" code 1204-852-70251.

Conflict of interest disclosure: The authors declare no conflicts of interest.

Permission to reproduce material from other sources: It was not necessary to obtain permissions to reproduce material from other sources.

Author Contributions: Conceptualization, D.M., C.E.G. and J.S.; methodology, D.M., C.E.G. and GHPF; software, D.M. and C.E.G.; validation, D.M., C.E.G. and J.S.; formal analysis, D.M., C.E.G., GHPF and J.S.; investigation, D.M., C.E.G. and J.S.; resources, J.S.; data curation, D.M. and C.E.G.; writing-original draft preparation, D.M.; writing-review and editing, D.M., C.E.G., GHPF and J.S.; visualization, D.M.; supervision, J.S.; project administration, J.S.; funding acquisition, J.S. All authors have read and agreed to the published version of the manuscript.

Clinical trial number: not applicable

References

1. Albright R, Benthuysen J, Cantin N, Caldeira K, Anthony K. Coral reef metabolism and carbon chemistry dynamics of a coral reef flat. Geophys Res Lett. 2015;42(10):3980–8. https://doi.org/10.1002/2015GL063488.
2. Al-Horani FA, Al-Moghrabi SM, de Beer D. The mechanism of calcification and its relation to photosynthesis and respiration in the scleractinian coral Galaxea fascicularis. Mar Biol. 2003a;142(3):419–26. https://doi.org/10.1007/s00227-002-0981-8.
3. Al-Horani FA, Al-Moghrabi SM, de Beer D. Microsensor study of photosynthesis and calcification in the scleractinian coral, *Galaxea fascicularis*: active internal carbon cycle. J Exp Mar Biol Ecol. 2003b;288(1):1–15. https://doi.org/10.1016/S0022-0981(02)00578-6.
4. Allemand D, Tambutté É, Zoccola D, Tambutté S. Coral Calcification, Cells to Reefs. Coral Reefs: An Ecosystem in Transition. Dordrecht: Springer; 2011. pp. 119–50.
5. Amado-Filho GM, Moura RL, Bastos AC, Salgado LT, Sumida PY, Guth AZ, et al. Rhodolith Beds Are Major CaCO3 Bio-Factories in the Tropical South West Atlantic. PLoS ONE. 2012;7(4):e35171. https://doi.org/10.1371/journal.pone.0035171.
6. Andersson AJ, Gledhill D. (2013). Ocean Acidification and Coral Reefs: Effects on Breakdown, Dissolution, and Net Ecosystem Calcification. *Annual Review of Marine Science*, 5(Volume 5, 2013), 321–348. https://doi.org/10.1146/annurev-marine-121211-172241
7. Anthony KRN, Hoegh-Guldberg O. Variation in coral photosynthesis, respiration and growth characteristics in contrasting light microhabitats: an analogue to plants in forest gaps and understoreys? Funct Ecol. 2003;17(2):246–59. https://doi.org/10.1046/j.1365-2435.2003.00731.x.
8. Atkinson M, Cuet P. Possible effects of ocean acidification on coral reef biogeochemistry: topics for research. Mar Ecol Prog Ser. 2008;373:249–56. https://doi.org/10.3354/meps07867.
9. Borowitzka MA, Larkum AWD. Calcification in algae: Mechanisms and the role of metabolism. CRC Crit Rev Plant Sci. 1987;6(1):1–45. https://doi.org/10.1080/07352688709382246.
10. Bracho-Villavicencio C, Matthews-Cascon H, García-Durán M, Vélez X, Lago N, Busquier L, et al. Benthic Colonization on New Materials for Marine Ecosystem Restoration in Porto Cesareo, Italy. J Mar Sci Eng. 2024;12(1). https://doi.org/10.3390/jmse12010169.
11. Carlot J, Rouzé H, Barneche DR, Mercière A, Espiau B, Cardini U, et al. Scaling up calcification, respiration, and photosynthesis rates of six prominent coral taxa. Ecol Evol. 2022;12(3):e8613. https://doi.org/10.1002/ece3.8613.
12. Carmona-Rodríguez A, Antón C, Climent M-Á, Garcés P, Montiel V, Ramos-Esplá AA. Sessile Biofouling on Electrolytic Carbonated Structures: Stages of Colonization and Succession. J Mar Sci Eng. 2024;12(3). https://doi.org/10.3390/jmse12030443.

13. Carreira-Flores D, Neto R, Ferreira HRS, Cabecinha E, Díaz-Agras G, Rubal M, et al. Colonization in Artificial Seaweed Substrates: Two Locations. One Year Diversity. 2023;15(6). https://doi.org/10.3390/d15060733.
14. de Carvalho RT, Wendt CHC, Willemes MJ, Bahia RdaG, Farina M, Salgado LT. Ontogeny and Early Steps of the Calcification Process in Coralline Algae Lithophyllum corallinae (Florideophyceae, Rhodophyta). Front Mar Sci. 2022;9. https://doi.org/10.3389/fmars.2022.900607.
15. Carvalho VF, Silva J, Kerr R, Anderson AB, Bastos EO, Cabral D, et al. When descriptive ecology meets physiology: a study in a South Atlantic rhodolith bed. Mar Biol Association United Kingd J Mar Biol Association United Kingd. 2020;100(3):347–60. https://doi.org/10.1017/S0025315420000284.
16. Chisholm JRM, Gattuso J-P. Validation of the alkalinity anomaly technique for investigating calcification of photosynthesis in coral reef communities. Limnol Oceanogr. 1991;36(6):1232–9. https://doi.org/10.4319/lo.1991.36.6.1232.
17. Cohen I, Dubinsky Z, Erez J. Light Enhanced Calcification in Hermatypic Corals: New Insights from Light Spectral Responses. Front Mar Sci. 2016. https://doi.org/10.3389/fmars.2015.00122. 2.
18. Cooley S, Schoeman D, Bopp L, Boyd P, Donner S, Ito S et al. (2022). Chapter 3: Oceans and Coastal Ecosystems and their Services. *IPCC AR6 WGII*. Available at: https://www.ipcc.ch/report/ar6/wg2/downloads/report/IPCC_AR6_WGII_FinalDraft_Chapter03.pdf [Accessed 9 August 2024].
19. Cooper TF, Ulstrup KE, Dandan SS, Heyward AJ, Kühl M, Muirhead A et al. (2010). Niche specialization of reef-building corals in the mesophotic zone: metabolic trade-offs between divergent Symbiodinium types. *Proceedings of the Royal Society B: Biological Sciences*, 278(1713), 1840–1850. https://doi.org/10.1098/rspb.2010.2321
20. Cornwall CE, Boyd PW, McGraw CM, Hepburn CD, Pilditch CA, Morris JN, et al. Diffusion Boundary Layers Ameliorate the Negative Effects of Ocean Acidification on the Temperate Coralline Macroalga Arthrocardia corymbosa. PLoS ONE. 2014;9(5):e97235. https://doi.org/10.1371/journal.pone.0097235.
21. Cornwall CE, Carlot J, Branson O, Courtney TA, Harvey BP, Perry CT, et al. Crustose coralline algae can contribute more than corals to coral reef carbonate production. Commun Earth Environ. 2023;4(1):1–12. https://doi.org/10.1038/s43247-023-00766-w.
22. Costa D, de Dolbeth A, Christoffersen M, Zúñiga-Upegui ML, Venâncio PT, M., de Lucena RFP. An Overview of Rhodoliths: Ecological Importance and Conservation Emergency. Life. 2023;13(7):1556. https://doi.org/10.3390/life13071556.
23. Cyronak T, Andersson AJ, Langdon C, Albright R, Bates NR, Caldeira K, et al. Taking the metabolic pulse of the world's coral reefs. PLoS ONE. 2018;13(1):e0190872. https://doi.org/10.1371/journal.pone.0190872.
24. Cyronak T, McMahon A, Eyre B. Carbon cycling hysteresis in permeable carbonate sands over a diel cycle: Implications for ocean acidification. Limnol Oceanogr. 2013;58:131–43. https://doi.org/10.4319/lo.2013.58.1.0131.

25. Dickson AG. Thermodynamics of the dissociation of boric acid in synthetic seawater from 273.15 to 318.15 K. Deep Sea Res Part Oceanogr Res Papers. 1990;37(5):755–66. https://doi.org/10.1016/0198-0149(90)90004-F.
26. Dickson AG, Millero FJ. A comparison of the equilibrium constants for the dissociation of carbonic acid in seawater media. Deep Sea Res Part Oceanogr Res Papers. 1987;34(10):1733–43. https://doi.org/10.1016/0198-0149(87)90021-5.
27. Dickson AG, Sabine CL, Christian JR. Guide to Best Practices for Ocean CO2 Measurements. North Pacific Marine Science Organization; 2007.
28. Doney SC, Fabry VJ, Feely RA, Kleypas JA. (2009). Ocean Acidification: The Other CO2 Problem. *Annual Review of Marine Science*, 1(Volume 1, 2009), 169–192. https://doi.org/10.1146/annurev.marine.010908.163834
29. Eyre BD, Andersson AJ, Cyronak T. Benthic coral reef calcium carbonate dissolution in an acidifying ocean. Nat Clim Change. 2014;4(11):969–76. https://doi.org/10.1038/nclimate2380.
30. Figueiredo M, Coutinho R, Villas-Boas A, Tâmega F, Mariath R. Deep-water rhodolith productivity and growth in the southwestern Atlantic. J Appl Phycol. 2012;24:497–493. https://doi.org/10.1007/s10811-012-9802-8.
31. Furla P, Galgani I, Durand I, Allemand D. Sources and Mechanisms of Inorganic Carbon Transport for Coral Calcification and Photosynthesis. J Exp Biol. 2000;203(22):3445–57. https://doi.org/10.1242/jeb.203.22.3445.
32. Gattuso J, Pichon M, Frankignoulle M. Biological control of air-sea CO2 fluxes: effect of photosynthetic and calcifying marine organisms and ecosystems. Mar Ecol Prog Ser. 1995;129:307–12. https://doi.org/10.3354/meps129307.
33. Gattuso J-P, Allemand D, Frakingnoulle M. Photosynthesis and Calcification at Cellular, Organismal and Community Levels in Coral Reefs: A Review on Interactions and Control by Carbonate Chemistry1. Am Zool. 1999;39(1):160–83. https://doi.org/10.1093/icb/39.1.160.
34. Gattuso JP, Allemand D, Frankignoulle M. Photosynthesis and Calcification at Cellular, Organismal and Community Levels in Coral Reefs: A Review on Interactions and Control by Carbonate Chemistry1. Am Zool. 1999;39(1):160–83. https://doi.org/10.1093/icb/39.1.160.
35. Gattuso JP, Frankignoulle M, Smith SV. (1999). Measurement of community metabolism and significance in the coral reef CO2 source-sink debate. *Proceedings of the National Academy of Sciences*, 96(23), 13017–13022. https://doi.org/10.1073/pnas.96.23.13017
36. Goh TZY, Bauman AG, Januchowski-Hartley FA, Morgan KM, Seah JCL, Todd PA. Growth and carbonate production of crustose coralline algae on a degraded turbid reef system. Mar Pollut Bull. 2021;173:113135. https://doi.org/10.1016/j.marpolbul.2021.113135.
37. Gómez CE, Acosta-Chaparro A, Bernal CA, Gómez-López DI, Navas-Camacho R, Alonso D. Seasonal Upwelling Conditions Modulate the Calcification Response of a Tropical Scleractinian Coral. Oceans. 2023;4(2):170–84. https://doi.org/10.3390/oceans4020012.

38. Gorbunov MY, Falkowski PG. Photoreceptors in the cnidarian hosts allow symbiotic corals to sense blue moonlight. Limnol Oceanogr. 2002;47(1):309–15. https://doi.org/10.4319/lo.2002.47.1.0309.
39. Goreau TF. The physiology of skeleton formation in corals. i. a method for measuring the rate of calcium deposition by corals under different conditions. Biol Bull. 1959;116(1):59–75. https://doi.org/10.2307/1539156.
40. Guinotte JM, Fabry VJ. Ocean acidification and its potential effects on marine ecosystems. Ann N Y Acad Sci. 2008;1134:320–42. https://doi.org/10.1196/annals.1439.013.
41. Gutner-Hoch E, Schneider K, Stolarski J, Domart-Coulon I, Yam R, Meibom A, et al. Evidence for Rhythmicity Pacemaker in the Calcification Process of Scleractinian Coral. Sci Rep. 2016;6(1):20191. https://doi.org/10.1038/srep20191.
42. Hofmann LC, Koch M, de Beer D. Biotic Control of Surface pH and Evidence of Light-Induced H+ Pumping and Ca2+-H+ Exchange in a Tropical Crustose Coralline Alga. PLoS ONE. 2016;11(7):e0159057. https://doi.org/10.1371/journal.pone.0159057.
43. Hofmann LC, Schoenrock K, de Beer D. Arctic Coralline Algae Elevate Surface pH and Carbonate in the Dark. Front Plant Sci. 2018;9. https://doi.org/10.3389/fpls.2018.01416.
44. Hurd CL. Water Motion, Marine Macroalgal Physiology, and Production. J Phycol. 2000;36(3):453–72. https://doi.org/10.1046/j.1529-8817.2000.99139.x.
45. Jardim V, l, Grall J, Barros-barreto M, beatriz, Bizien A, Benoit T, Braga J, c, et al. A Common Terminology to Unify Research and Conservation of Coralline Algae and the Habitats They Create. Aquat Conservation-marine Freshw Ecosyst. 2025;35(3). https://doi.org/10.1002/aqc.70121.
46. Jokiel PL, Jury CP, Rodgers KS. Coral-algae metabolism and diurnal changes in the CO2-carbonate system of bulk sea water. PeerJ. 2014;2:e378. https://doi.org/10.7717/peerj.378.
47. Kamenos NA, Burdett HL, Aloisio E, Findlay HS, Martin S, Longbone C, et al. Coralline algal structure is more sensitive to rate, rather than the magnitude, of ocean acidification. Glob Change Biol. 2013;19(12):3621–8. https://doi.org/10.1111/gcb.12351.
48. Kleypas JA, Feely RA, Fabry VJ, Langdon C, Robbins L. Impacts of Ocean Acidification on Coral Reefs and Other Marine Calcifiers: A Guide for Future Research. St Petersburg: NSF, NOAA and the USGS; 2006.
49. Kuffner IB, Hickey TD, Morrison JM. Calcification rates of the massive coral Siderastrea siderea and crustose coralline algae along the Florida Keys (USA) outer-reef tract. Coral Reefs. 2013;32(4):987–97. https://doi.org/10.1007/s00338-013-1047-8.
50. Kuhl, M., hl, Cohen, Y., Dalsgaard, T., Jø, B.B., rgensen, et al. (1995). Microenvironment and photosynthesis of zooxanthellae in scleractinian corals studied with microsensors for O2, pH and light. *Marine Ecology Progress Series*, 117, 159–172. https://doi.org/10.3354/meps117159.
51. Larkum AWD, Grossman AR, Raven JA, editors. Photosynthesis in Algae: Biochemical and Physiological Mechanisms. Springer International Publishing: Cham; 2020.
52. Lee K, Millero FJ, Byrne RH, Feely RA, Wanninkhof R. The recommended dissociation constants for carbonic acid in seawater. Geophys Res Lett. 2000;27(2):229–32.

https://doi.org/10.1029/1999GL002345.

53. Legrand E, Riera P, Lutier M, Coudret J, Grall J, Martin S. Species interactions can shift the response of a maerl bed community to ocean acidification and warming. Biogeosciences. 2017;14(23):5359–76. https://doi.org/10.5194/bg-14-5359-2017.
54. Lenth RV, Banfai B, Bolker B, Buerkner P, Giné-Vázquez I, Herve M et al. (2025). emmeans: Estimated Marginal Means, aka Least-Squares Means.
55. Leung JYS, Zhang S, Connell SD. Is Ocean Acidification Really a Threat to Marine Calcifiers? A Systematic Review and Meta-Analysis of 980 + Studies Spanning Two Decades. Small. 2022;18(35):e2107407. https://doi.org/10.1002/smll.202107407.
56. Levy O, Appelbaum L, Leggat W, Gothlif Y, Hayward DC, Miller DJ, et al. Light-Responsive Cryptochromes from a Simple Multicellular Animal, the Coral Acropora millepora. Science. 2007;318(5849):467–70. https://doi.org/10.1126/science.1145432.
57. Lirman D, Manzello D. Patterns of resistance and resilience of the stress-tolerant coral *Siderastrea radians* (Pallas) to sub-optimal salinity and sediment burial. J Exp Mar Biol Ecol. 2009;369(1):72–7. https://doi.org/10.1016/j.jembe.2008.10.024.
58. MacDonald E, Byrne M, Deaker DJ, Foster GL, Gabarda ST, MacDonald J et al. (2025). Timing of calcification and environmental variability determine pH proxy fidelity in coastal calcifying macroalgae. *Limnology and Oceanography*, n/a(n/a). https://doi.org/10.1002/lno.70124
59. Macreadie PI, Costa MDP, Atwood TB, Friess DA, Kelleway JJ, Kennedy H, et al. Blue carbon as a natural climate solution. Nat Reviews Earth Environ. 2021;2(12):826–39. https://doi.org/10.1038/s43017-021-00224-1.
60. Mallela J. Calcification by Reef-Building Sclerobionts. PLoS ONE. 2013;8(3):e60010. https://doi.org/10.1371/journal.pone.0060010.
61. Mallela J, Perry CT. Calcium carbonate budgets for two coral reefs affected by different terrestrial runoff regimes, Rio Bueno, Jamaica. Coral Reefs. 2007;26(1):129–45. https://doi.org/10.1007/s00338-006-0169-7.
62. Mallela J, Milne BC, Martinez-Escobar D. A comparison of epibenthic reef communities settling on commonly used experimental substrates: PVC versus ceramic tiles. J Exp Mar Biol Ecol. 2017;486:290–5. https://doi.org/10.1016/j.jembe.2016.10.028.
63. Mallon J, Cyronak T, Hall ER, Banaszak AT, Exton DA, Bass AM. Light-driven dynamics between calcification and production in functionally diverse coral reef calcifiers. Limnol Oceanogr. 2022;67(2):434–49. https://doi.org/10.1002/lno.12002.
64. Mao J, Burdett H, Kamenos N. Efficient carbon recycling between calcification and photosynthesis in red coralline algae. Biol Lett. 2024;20:20230598. https://doi.org/10.1098/rsbl.2023.0598.
65. Martin S, Cohu S, Vignot C, Zimmerman G, Gattuso J-P. One-year experiment on the physiological response of the Mediterranean crustose coralline alga, Lithophyllum cabiochae, to elevated pCO2 and temperature. Ecol Evol. 2013;3(3):676–93. https://doi.org/10.1002/ece3.475.

66. McCoy SJ, Pueschel CM, Cornwall CE, Comeau S, Kranz SA, Spindel NB, et al. Calcification in the coralline red algae: a synthesis. Phycologia. 2023;62(6):648–66. https://doi.org/10.1080/00318884.2023.2285673.
67. McNicholl C, Koch MS, Hofmann LC. Photosynthesis and light-dependent proton pumps increase boundary layer pH in tropical macroalgae: A proposed mechanism to sustain calcification under ocean acidification. J Exp Mar Biol Ecol. 2019;521:151208. https://doi.org/10.1016/j.jembe.2019.151208.
68. Mehrbach C, Culberson CH, Hawley JE, Pytkowicx RM. Measurement of the Apparent Dissociation Constants of Carbonic Acid in Seawater at Atmospheric Pressure. Limnol Oceanogr. 1973;18(6):897–907. https://doi.org/10.4319/lo.1973.18.6.0897.
69. Mos B, Holloway C, Kelaher BP, Santos IR, Dworjanyn SA. Alkalinity of diverse water samples can be altered by mercury preservation and borosilicate vial storage. Sci Rep. 2021;11(1):9961. https://doi.org/10.1038/s41598-021-89110-w.
70. Noisette F, Duong G, Six C, Davoult D, Martin S. Effects of elevated pCO2 on the metabolism of a temperate rhodolith Lithothamnion corallioides grown under different temperatures. J Phycol. 2013a;49(4):746–57. https://doi.org/10.1111/jpy.12085.
71. Noisette F, Egilsdottir H, Davoult D, Martin S. Physiological responses of three temperate coralline algae from contrasting habitats to near-future ocean acidification. J Exp Mar Biol Ecol. 2013b;448:179–87. https://doi.org/10.1016/j.jembe.2013.07.006.
72. Perkol-Finkel S, Benayahu Y. Differential recruitment of benthic communities on neighboring artificial and natural reefs. J Exp Mar Biol Ecol. 2007;340(1):25–39. https://doi.org/10.1016/j.jembe.2006.08.008.
73. Pessarrodona A, Attlan O, Wernberg T. Significant carbonate production on a temperate reef system in southwestern Australia. Mar Environ Res. 2025;211:107416. https://doi.org/10.1016/j.marenvres.2025.107416.
74. Pierrot DE, Lewis E, Wallace DWR, Wallace DWR. (2006). MS Excel Program Developed for CO2 System Calculations.
75. de Romanó M, Koweek DA, Cyronak T, Takeshita Y, Griffin A, Wolfe K, et al. Unexpected role of communities colonizing dead coral substrate in the calcification of coral reefs. Limnol Oceanogr. 2021;66(5):1793–803. https://doi.org/10.1002/lno.11722.
76. Ross CL, Warnes A, Comeau S, Cornwall CE, Cuttler MVW, Naugle M, et al. Coral calcification mechanisms in a warming ocean and the interactive effects of temperature and light. Commun Earth Environ. 2022;3(1):72. https://doi.org/10.1038/s43247-022-00396-8.
77. Sabine CL, Feely RA, Gruber N, Key RM, Lee K, Bullister JL, et al. The Oceanic Sink for Anthropogenic CO2. Science. 2004;305(5682):367–71. https://doi.org/10.1126/science.1097403.
78. Sajid S, Zhang G, Zhang Z, Chen L, Lu Y, Fang JK-H, et al. Comparative analysis of biofilm bacterial communities developed on different artificial reef materials. J Appl Microbiol. 2024;135(11):lxae268. https://doi.org/10.1093/jambio/lxae268.

79. Sánchez JA, Murgueitio A, Rivera-Forero C, Marín-Casas DH, Gómez CE. Tropical reefs in the aftermath of climate change. Discover Conserv. 2025;2(1):23. https://doi.org/10.1007/s44353-025-00044-0.
80. Schmidt CA, Stifler CA, Luffey EL, Fordyce BI, Ahmed A, Pujol B, G., et al. Faster Crystallization during Coral Skeleton Formation Correlates with Resilience to Ocean Acidification. J Am Chem Soc. 2022;144(3):1332–41. https://doi.org/10.1021/jacs.1c11434.
81. Schubert N, Hofmann LC, Almeida Saá AC, Moreira AC, Arenhart RG, Fernandes CP, et al. Calcification in free-living coralline algae is strongly influenced by morphology: Implications for susceptibility to ocean acidification. Sci Rep. 2021;11(1):11232. https://doi.org/10.1038/s41598-021-90632-6.
82. Schubert N, Peña V, Salazar VW, Horta PA, Neves P, Ribeiro C, et al. Rhodolith Physiology Across the Atlantic: Towards a Better Mechanistic Understanding of Intra- and Interspecific Differences. Front Mar Sci. 2022;9. https://doi.org/10.3389/fmars.2022.921639.
83. Schubert N, Salazar VW, Rich WA, Vivanco Bercovich M, Saá A, Fadigas AC, S.D., et al. Rhodolith primary and carbonate production in a changing ocean: The interplay of warming and nutrients. Sci Total Environ. 2019;676:455–68. https://doi.org/10.1016/j.scitotenv.2019.04.280.
84. Schubert N, Tuya F, Peña V, Horta PA, Salazar VW, Neves P, et al. Pink power—the importance of coralline algal beds in the oceanic carbon cycle. Nat Commun. 2024;15(1):8282. https://doi.org/10.1038/s41467-024-52697-5.
85. Simancas-Giraldo SM, Xiang N, Kennedy MM, Nafeh R, Zelli E, Wild C. Photosynthesis and respiration of the soft coral Xenia umbellata respond to warming but not to organic carbon eutrophication. PeerJ. 2021;9:e11663. https://doi.org/10.7717/peerj.11663.
86. Singmann H, Bolker B, Westfall J, Aust F, Ben-Shachar MS, Højsgaard S et al. (2024). afex: Analysis of Factorial Experiments.
87. Sneed JM, Campbell JE, Looby A, Giorgi A, Paul VJ. Varying effects of climate change on the photosynthesis and calcification of crustose coralline algae: Implications for settlement of coral larvae. Clim Change Ecol. 2025;9:100090. https://doi.org/10.1016/j.ecochg.2024.100090.
88. Sordo L, Santos R, Barrote I, Freitas C, Silva J. Seasonal Photosynthesis, Respiration, and Calcification of a Temperate Maërl Bed in Southern Portugal. Front Mar Sci. 2020. https://doi.org/10.3389/fmars.2020.00136. 7.
89. Sordo L, Santos R, Barrote I, Silva J. High CO2 decreases the long-term resilience of the free-living coralline algae Phymatolithon lusitanicum. Ecol Evol. 2018;8(10):4781–92. https://doi.org/10.1002/ece3.4020.
90. Suzuki A, Nakamori T, Kayanne H. The mechanism of production enhancement in coral reef carbonate systems: model and empirical results. Sed Geol. 1995;99(3):259–80. https://doi.org/10.1016/0037-0738(95)00048-D.
91. Tuya F, Schubert N, Aguirre J, Basso D, Bastos EO, Berchez F, et al. Levelling-up rhodolith-bed science to address global-scale conservation challenges. Sci Total Environ. 2023;892:164818.

https://doi.org/10.1016/j.scitotenv.2023.164818.

92. Venn AA, Tambutté E, Caminiti-Segonds N, Techer N, Allemand D, Tambutté S. Effects of light and darkness on pH regulation in three coral species exposed to seawater acidification. Sci Rep. 2019;9(1):2201. https://doi.org/10.1038/s41598-018-38168-0.
93. Wang L, Liang Z, Lu D, Lv S, Li Z, Tan R, et al. Artificial reefs promote coastal carbon stabilization potential through hydrological condition and microbial pathways. Water Res. 2026;294:125502. https://doi.org/10.1016/j.watres.2026.125502.
94. Wickham H. (2016). *ggplot2*. Springer International Publishing: Cham.
95. Wilking LE, Dillon KS, Rakocinski CF. Artificial reef biofouling community impacts on ecosystem metabolism and biogeochemical cycling in estuarine waters of the northern Gulf of Mexico. Estuar Coast Shelf Sci. 2023;295:108555. https://doi.org/10.1016/j.ecss.2023.108555.
96. Wooldridge SA. (2010). Is the coral-algae symbiosis really 'mutually beneficial' for the partners? *BioEssays*, 32(7), 615–625. https://doi.org/10.1002/bies.200900182
97. Yanovski R, Barak H, Brickner I, Kushmaro A, Abelson A. The microbial community of coral reefs: biofilm composition on artificial substrates under different environmental conditions. Mar Biol. 2024;171(3):74. https://doi.org/10.1007/s00227-024-04400-x.

Figures

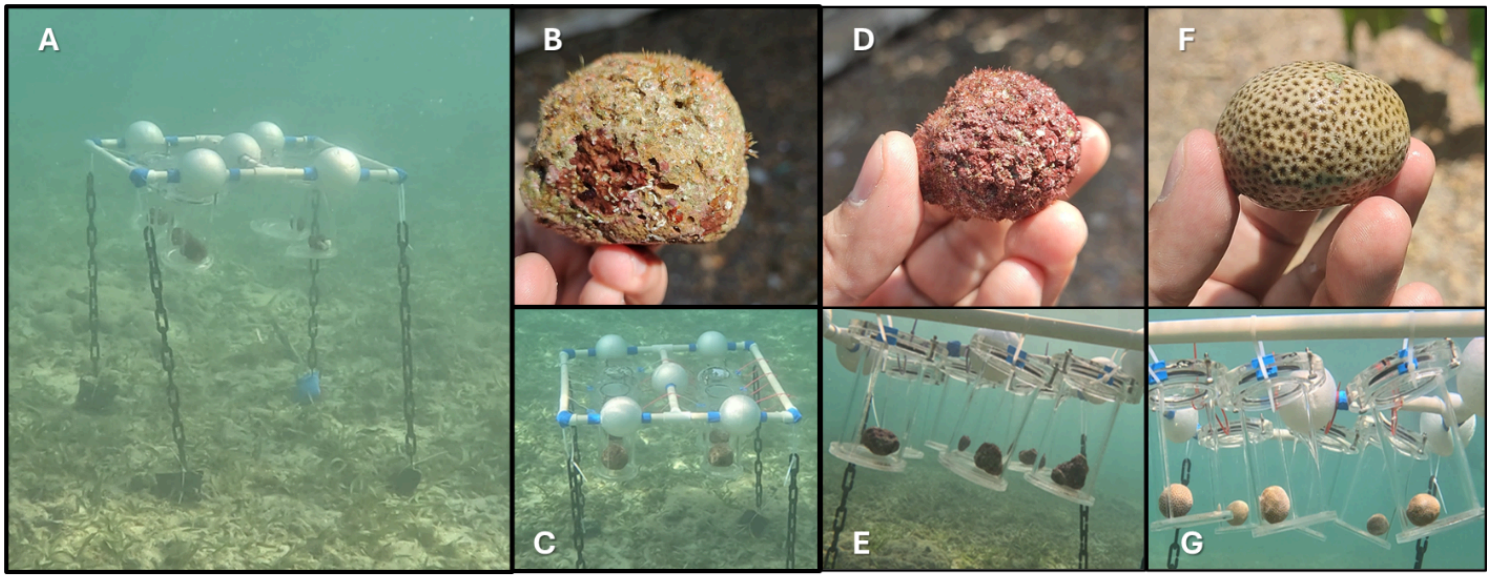


Figure 1

Experimental in situ incubation system and functional units used in the study. (A) Pendulant table-type experimental deployment with suspended acrylic incubation chambers. (B) Artificial substrate colonized by benthic organisms. (C) Underwater view of incubation chambers containing colonized artificial substrates. (D) Rhodoliths (nucleated crustose coralline algal nodules) collected from the fringing reef. (E) Underwater view of incubation chambers containing rhodoliths. (F) Coralith: a spherical colony of

Siderastrea radians from a seagrass meadow. (G) Underwater view of incubation chambers containing *S. radians* colonies.

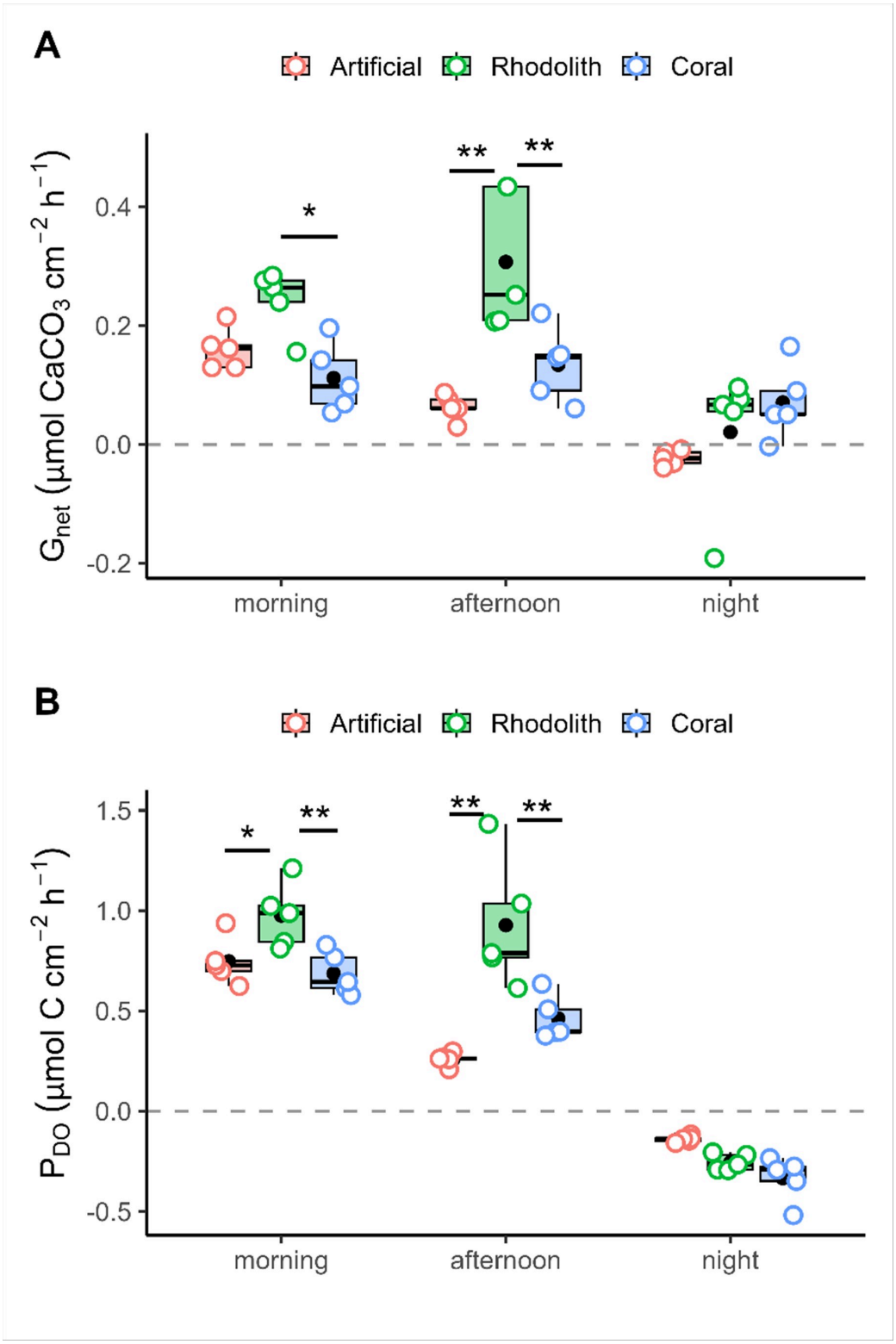


Figure 2

Diel metabolic rates (morning, afternoon, and night) in colonized artificial substrates, rhodoliths and corals. (A) net calcification rates (G_{net}, µmol $CaCO_3$ cm^{-2} h^{-1}) and (B) Net organic carbon production

rates (P_{DO}, µmol C cm^{-2} h^{-1}), recorded during morning, afternoon, and night periods. Plots show median (black circle) and IQR (whisker), mean (horizonal bars) and individual data points are represented as empty circles. Asterisks and horizontal lines below indicate statistically significant differences (P-value 0.01–0.001 **, 0.05–0.01 *) between groups.

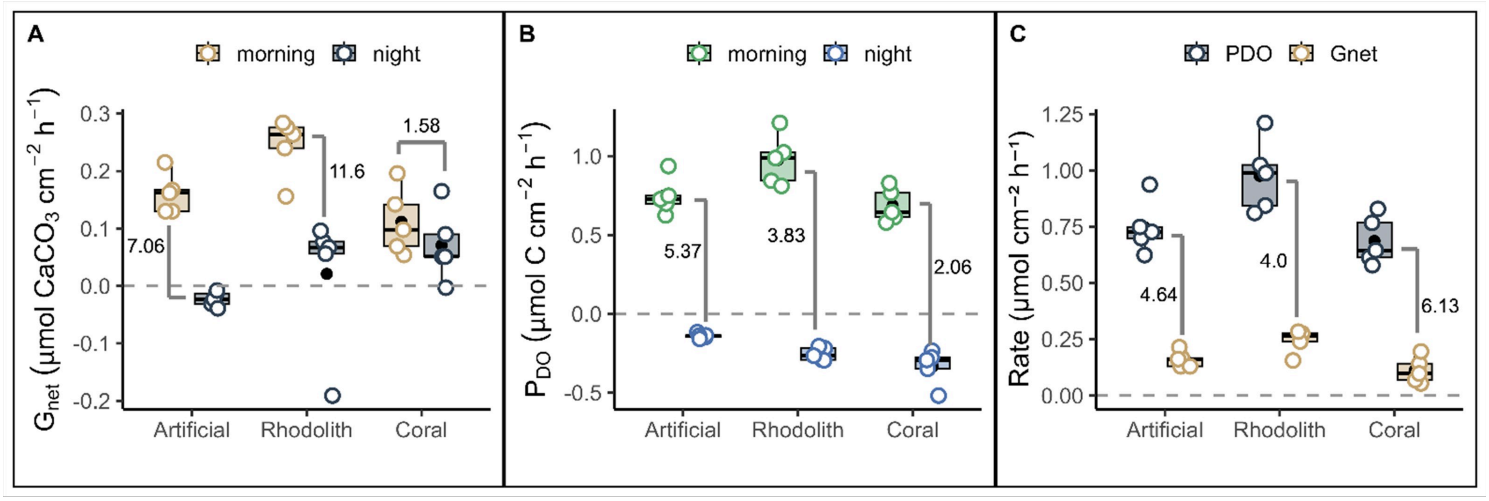


Figure 3

Comparison of metabolic rates: morning and night net calcification (A), net organic carbon production (P_{DO}, morning) vs. net respiratory carbon loss (P_{DO}, night) (B), and light organic carbon production to net calcification rates ratios (C) between all functional units. Grey lines and numbers indicate the |morning/night| ratios in panels A and B, and the P_{DO}/G_{net} ratio in panel C.

Supplementary Files

This is a list of supplementary files associated with this preprint. Click to download.

- SupplementaryMaterialsinfo.docx
- SupplementarymaterialDC30526smt.docx